CHEMISTRY OF MATERIALS

pubs.acs.org/cm

Article

Synthetic Antifreeze Glycoproteins with Potent Ice-Binding Activity

Anna C. Deleray, Simranpreet S. Saini, Alexander C. Wallberg, and Jessica R. Kramer*

Cite This: *Chem. Mater.* 2024, 36, 3424−3434

Read Online

ACCESS | Metrics & More | Article Recommendations | Supporting Information

ABSTRACT: Antifreeze glycoproteins (AFGPs) are produced by extremophiles to defend against tissue damage in freezing climates. Cumbersome isolation from polar fish has limited probing AFGP molecular mechanisms of action and limited development of bioinspired cryoprotectants for application in agriculture, foods, coatings, and biomedicine. Here, we present a rapid, scalable, and tunable route to synthetic AFGPs (sAFGPs) using *N*-carboxyanhydride polymerization. Our materials are the first mimics to harness the molecular size, chemical motifs, and long-range conformation of native AFGPs. We found that ice-binding activity increases with chain length, Ala is a key residue, and the native protein sequence is not required. The glycan structure had only minor effects, and all glycans examined displayed antifreeze activity. The sAFGPs are biodegradable, nontoxic, internalized into endocytosing cells, and bystanders in cryopreservation of human red blood cells. Overall, our sAFGPs functioned as surrogates for bona fide AFGPs, solving a long-standing challenge in accessing natural antifreeze materials.

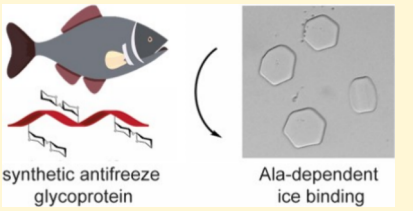

INTRODUCTION

Extremophile organisms in subzero climates produce specialized antifreeze proteins to protect their tissues from freezing damage.[1−4] These proteins bind to ice to lower plasma's freezing point and modify ice crystal shape and size to prevent mechanical damage to tissues.[5−8] Antifreeze proteins are of great interest for applications in food technology, agriculture, fisheries, coatings, and in the petroleum industry.[9,10] They have even come to market as texture-improving ice cream additives.[11] A particularly impactful potential application is to improve post-thaw tissue viability and function in biomedical cryopreservation.[12,13]

To date, many antifreeze proteins have been identified, including a subgroup called antifreeze glycoproteins (AFGPs), which are highly potent ice-shaping molecules.[14,15] Identified as the major serum protein of certain Antarctic and Arctic fish, AFGPs are a fascinating and rare example of convergent evolution.[16] AFGPs consist of a highly conserved Ala-Ala-Thr repeat, with Thr bearing the disaccharide βGal(1→3)αGalNAc (Figure 1A).[7] Isoforms from 2.6 to 33.7 kDa, classified as AFGP8−AFGP1, are encoded within polyprotein genes.[16] Circular dichroism (CD), nuclear magnetic resonance (NMR), Fourier transformed infrared spectroscopy (FTIR), and computational modeling have all been utilized to characterize AFGP conformation.[17−20] AFGPs adopt a variety of solution conformations including disordered, β-turn, extended, and helical structures that are spectroscopically similar to the polyproline type II (PPII) conformation[21,22] observed in Pro-rich proteins like collagen and mucins[23] (Figure 1A). Spectroscopic signatures for the PPII structure increase upon cooling, and modeling indicates that the helix might be important for ice binding. A true PPII-helix is left-handed, has three residues/turn, and a helical pitch of 9.3 Å.[21,22] It is still unclear whether native AFGPs adopt identical long-range helical spacing.

AFGPs possess two well-established properties: ice recrystallization inhibition (IRI) and thermal hysteresis (TH). IRI prevents the growth of large ice crystals, while TH produces a noncolligative freezing point depression and gap between solution freezing and melting points.[6,8] Effects are observable at concentrations 300−100,000× lower than dissolved salts and sugars.[24] Overall, these properties render AFGPs highly attractive for cryopreservation applications in biomedical, agricultural, and food sectors.[9−13]

Despite their potential, there are no commercial AFGP sources. Isolating the proteins requires a polar fishing trip followed by labor-intensive fractionation that still yields heterogeneous mixtures of isoforms and potential contamination with strong allergens.[15] Additionally, high molecular weight (MW) native AFGPs (50−150 residues, 10.5−34 kDa) are much more active than low MW AFGPs (12−38 residues, 2.6−7.9 kDa) but are of low abundance.[6,8,15,25] The proteins have so far resisted recombinant production.[9,10,26] Synthetic approaches using solid-phase synthesis or step-growth polymerizations have been beautifully explored but are laborious and limited to low-activity, low-MW AFGPs.[10,18,27−38] Additionally, many structures utilized non-native residues or glycans that could affect biocompatibility. Poly(vinyl alcohol) (PVA) has been investigated as a

Received: January 29, 2024
Revised: March 13, 2024
Accepted: March 15, 2024
Published: March 25, 2024

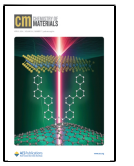

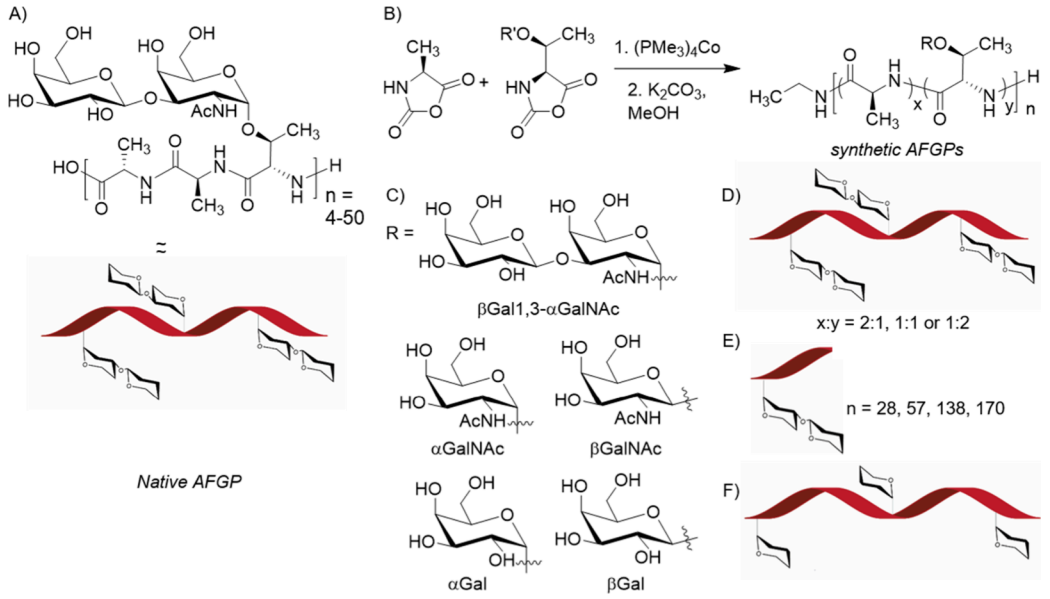

Figure 1. Structure of native AFGPs and preparation of the sAFGP panel. (A) Chemical structure of the AFGP tripeptide repeat and native PPII-type helical conformation. (B) Preparation of tunable sAFGPs by NCA polymerization using transition metal catalysis. (C) Structures of the five glycans utilized in the sAFGP panel. sAFGPs were prepared with varying (D) ratios of Ala:glycoThr, (E) molecular weights, and (F) glycans.

polyhydroxylated surrogate,[39] while polyproline has been utilized to capture the PPII conformation.[40] These structures are reportedly orders of magnitude less active than even low MW AFGPs. PVA has shown mixed results in combination with traditional cryoprotectants.[39,41,42] Various other mimics have been investigated but have shown little or no IRI activity.[26,36,43−47]

A need remains for an accessible route to AFGPs, which allows molecular tuning to probe the characteristics that drive ice binding. Here, we present a rapid, scalable, and tunable route to synthetic AFGPs (sAFGPs) using amino acid *N*-carboxyanhydride (NCA) polymerization (Figure 1B−F). Our building blocks were prepared on a gram scale, and the NCA method is used commercially.[48] The approach allows precise control over polypeptide backbone MW, composition, and glycosylation.[49,50] We tuned these factors to optimize activity and to reveal long-debated molecular drivers of antifreeze activity. Finally, we probed the interaction of sAFGPs with model biological systems.

RESULTS AND DISCUSSION

Design and Synthesis of the sAFGP Panel. Despite nearly 70 years of study, the molecular details of AFGP ice binding are debated. The generally accepted mechanism involves a protein ice-binding face and a nonbinding face.[51−53] After adsorption to an embryonic ice crystal, the nonbinding face prevents ordering of approaching liquid water molecules, resulting in inhibited crystal growth, ice shaping, and lowered melting point. However, the roles of hydrophobic Ala versus hydrophilic sugars in these faces are unclear.

Molecular dynamics modeling of a 14-residue AFGP predicted, while many binding configurations are allowed, the PPII structure is preferred and that the driving force is that Ala methyl groups nest into ice-surface cavities driven by the entropy of dehydration.[54] An alternative model proposed amphipathic binding where Ala methyl groups and glycan hydroxyls cooperatively bind ice.[55] Ice binding via the hydroxyls alone has also been proposed based on observation of fluorescently labeled AFGPs on ice crystal surfaces, and because the activity was disrupted by sugar-complexing borate.[5,6,56,57] Additionally, AFGPs adsorb more efficiently to hydrophilic surfaces[58,59] and monolayers of βGal(1→3)-αGalNAc alone shape ice.[60]

Prior work indicated loss of activity due to oxidation, alkylation, and borylation of AFGP disaccharides.[14,61,62] Tachibana conducted the most comprehensive study of glycan structure to date.[38] They compared 6−9 residue AFGP fragments bearing the α- vs β-linked native disaccharide, αGal vs αGalNAc, and other glycans. They observed significant differences in TH and IRI behavior and identified the α-linkage and C2 NHAc group as particularly important for activity. However, their peptides could only make 2−3 PPII-helical turns, and this assumes end-group participation. Experimental evidence using native AFGPs indicates that the activity is strongly dependent upon MW. However, data are convoluted since, due to purification challenges, experiments were conducted on pooled fractions.

To explore AFGP structure−function, we synthesized sAFGPs via NCA polymerization using our established methods.[49,50] We varied the chain length, glycosylation pattern, and hydrophobicity (Figure 1B−F). To explore the role of MW, 28−170mers were prepared (Figure 1E). To probe the role of Ala methyl groups vs glycan hydroxyls, we prepared glycopolypeptides with varied densities of the two residues. The native amino acid ratio of 2:1 Ala:Thr was increased to 1:1 or 1:2 (Figure 1D).

To explore glycosylation's role in extended PPII-type structure and sAFGP antifreeze activity, we prepared glyco-Thr conjugates bearing αGal, βGal, αGalNAc, βGalNAc, or native disaccharide βGal(1,3)αGalNAc (abbreviated as βGalαGalNAc) (Figure 1C,F). These glycans might differently affect hydrogen bonding or protein secondary structure.[50,63,64] NMR studies on short αGalNAc-Thr/Ser peptides suggested that an intramolecular hydrogen bond between the sugar *N*-Ac and Thr carbonyl is a stabilizing force for the PPII structure. However, our recent CD studies of high MW glycosylated

https://doi.org/10.1021/acs.chemmater.4c00266
Chem. Mater. 2024, 36, 3424−3434

polyThr indicated that the PPII conformation is adopted in structures lacking the *N*-Ac group (i.e., Gal instead of GalNAc).

Ala NCA was prepared from Ala in one step by treatment with phosgene in tetrahydrofuran (THF).[49] Peracetylated glyco-Thr conjugates were prepared using literature protocols (See Supporting Information (SI)).[30,50,65] All conjugates were converted to NCAs from their *tert*-butyloxycarbonyl-forms by treatment with triphosgene and triethylamine in THF, via our previously optimized conditions.[50] Direct phosgenation of glyco-Thrs in the same manner as for Ala results in poor yields. In all cases, NCAs were isolated by anhydrous chromatography to give crystalline monomer.[66]

Glyco-Thr and Ala NCAs were converted to sAFGPs using the $(PMe_3)_4Co$ catalyst in THF (Figure 1B). This catalyst was chosen since it offers fast initiation kinetics with suppression of side reactions, resulting in formation of high MW polymers of low dispersity.[67−69] The initiation mechanism has also been studied in detail and is known to result in the initiation site end group derived from the amino acid chain and α carbon, as drawn in Figure 1 for Ala.[67,70] NCA:catalyst ratios were varied to tune the degree of polymerization (DP), and monomer feed ratios were varied to tune composition. Complete monomer consumption was evidenced by infrared spectroscopy. NCA carbonyl stretches at ∼1850 and 1790 cm^{-1} disappeared, while peptide carbonyl stretches at ∼1650 and 1540 cm^{-1} emerged (see the SI). Peracetylated sAFGPs were characterized by ^{1}H NMR and size exclusion chromatography in dimethylformamide (DMF) plus 0.1 M LiBr, coupled to multiangle light scattering and refractive index (SEC/MALS/RI) (Figure 2A, Table 1, see the SI). MW and DP correlated well with the expected values. Samples bearing disaccharides had good solubility in DMF and could be analyzed by SEC/MALS/RI in peracetylated form. Samples bearing monosaccharides were insufficiently soluble in DMF and were therefore analyzed by SEC/MALS/RI in deacetylated form in Dulbecco's phosphate buffered saline (DPBS). Samples were also analyzed by end group analysis by ^{1}H NMR using previously published methods.[49,71] See the SI for representative spectra and MALS traces.

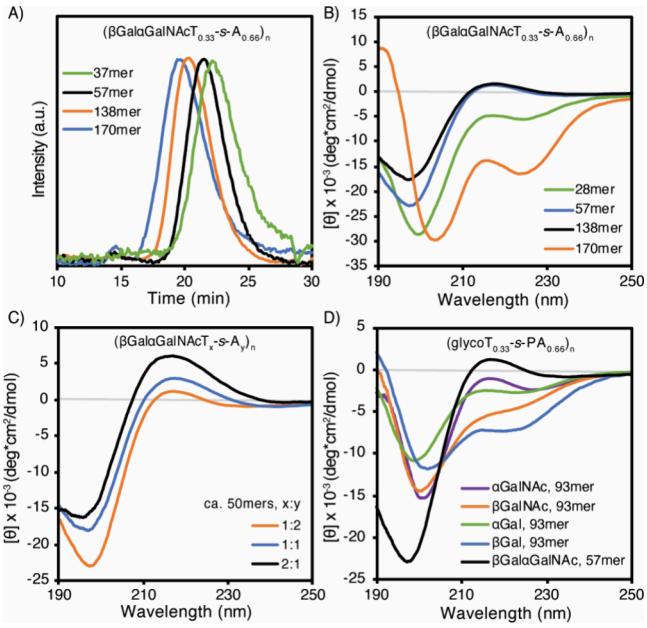

Figure 2. Characterization of sAFGP molar masses and conformations. (A) SEC/MALS/RI in dimethylformamide with 0.1 M LiBr, indicating differing elution times for peracetylated chains of increasing lengths. (B−D) Aqueous CD spectra of deacetylated sAFGPs where (B) are structures with increasing molecular weights, (C) are structures with increasing βGalαGalNAcThr content, and (D) are structures bearing glycans of differing identity and anomeric orientation.

Table 1. Representative Data for Characterization of sAFGP Polymers Prepared Using $(PMe_3)_4Co$ in THF[a]

sAFGP[a]	M_n	Đ	DP[d]
$(\beta GalT_{0.33}\text{-}s\text{-}A_{0.66})_n$	17,680[b]	1.54[b]	93
$(\alpha GalT_{0.33}\text{-}s\text{-}A_{0.66})_n$	17,680[b]	1.33[b]	93
$(\beta GalNAcT_{0.33}\text{-}s\text{-}A_{0.66})_n$	17,649[b]	1.65[b]	93
$(\alpha GalNAcT_{0.33}\text{-}s\text{-}A_{0.66})_n$	17,649[b]	1.21[b]	93
$(\beta Gal\alpha GalNAcT_{0.33}\text{-}s\text{-}A_{0.66})_n$	8,134[c]	1.81[c]	28
$(\beta Gal\alpha GalNAcT_{0.33}\text{-}s\text{-}A_{0.66})_n$	16,460[c]	1.27[c]	57
$(\beta Gal\alpha GalNAcT_{0.33}\text{-}s\text{-}A_{0.66})_n$	39,680[c]	1.17[c]	138
$(\beta Gal\alpha GalNAcT_{0.33}\text{-}s\text{-}A_{0.66})_n$	48,830[c]	1.39[c]	170
$(\beta Gal\alpha GalNAcT_{0.5}\text{-}s\text{-}A_{0.5})_n$	20,490[c]	1.47[c]	52
$(\beta Gal\alpha GalNAcT_{0.66}\text{-}s\text{-}A_{0.33})_n$	23,140[c]	1.31[c]	46

[a][a]Sample name and amino acid composition. [b,c] M_n (number average molecular weight) and Đ (dispersity) as determined by SEC/MALS/RI in [b] DPBS for polymers analyzed in their deacetylated forms or [c] in DMF with 0.1M LiBr for polymers analyzed in their peracetylated forms. [b,c] ^{1}H NMR was also used to confirm the structure and M_n. [d] Observed degree of polymerization (DP).

Overall, we found that the NCA method offers a rapid, scalable, and convenient route to sAFGPs of a tunable structure. Glycopolypeptides that are on par with the molar masses of the native fish proteins are readily produced and are free of the potential of contamination with strong allergens.

Characterization of the sAFGP Structure. Circular dichroism (CD) was used to characterize the sAFGP secondary structures. Distinct signatures are observed for the $\eta \rightarrow \pi^*$ and $\pi \rightarrow \pi^*$ transitions of PPII, disordered, sheet, or α-helical conformations.[72−75] Homopolymers of βGalNAc- or βGalαGalNAcThr have not been previously prepared; however, our previous work on αGalNAc-, αGal-, and βGal-bearing polyThr revealed that they adopt extended PPII-like conformations.[50] We should note that it can be challenging to distinguish between true PPII and extended peptide conformations.[76] The αGalNAc amide positive ellipticity between 190 and 200 nm overlaps with the peptide $\pi \rightarrow \pi^*$ transition.[50]

For sAFGPs with native 1:2 Thr:Ala and βGalαGalNAc, MW-dependent secondary structures were observed (Figure 2B). The 28mer (equivalent to AFGP7−AFGP6) exhibited a combination of disordered and PPII-type conformations as evidenced by minor absorbance at ∼217 nm in the PPII region and spectral alignment with denatured collagen and intrinsically disordered proteins.[74,75] This was expected considering that the 28mer can only make ∼9 PPII-helical turns. Helical propensity increases with chain length,[23,49] which explains the classic PPII structure observed for 57- and 138-mers (maxima at ∼217 nm, minima at ∼197 nm). Our spectra correlate nicely with those of native AFGP5−AFGP2.[21,30,62] Spectra obtained in water and phosphate buffered saline (PBS) were identical, and sAFGP conformation was stable from 4−50 °C (see the SI).

The disaccharide-sAFGP 170mer adopted a mix of PPII- and presumably α-helices (minimum shift to 203 nm and new

https://doi.org/10.1021/acs.chemmater.4c00266
Chem. Mater. 2024, 36, 3424−3434

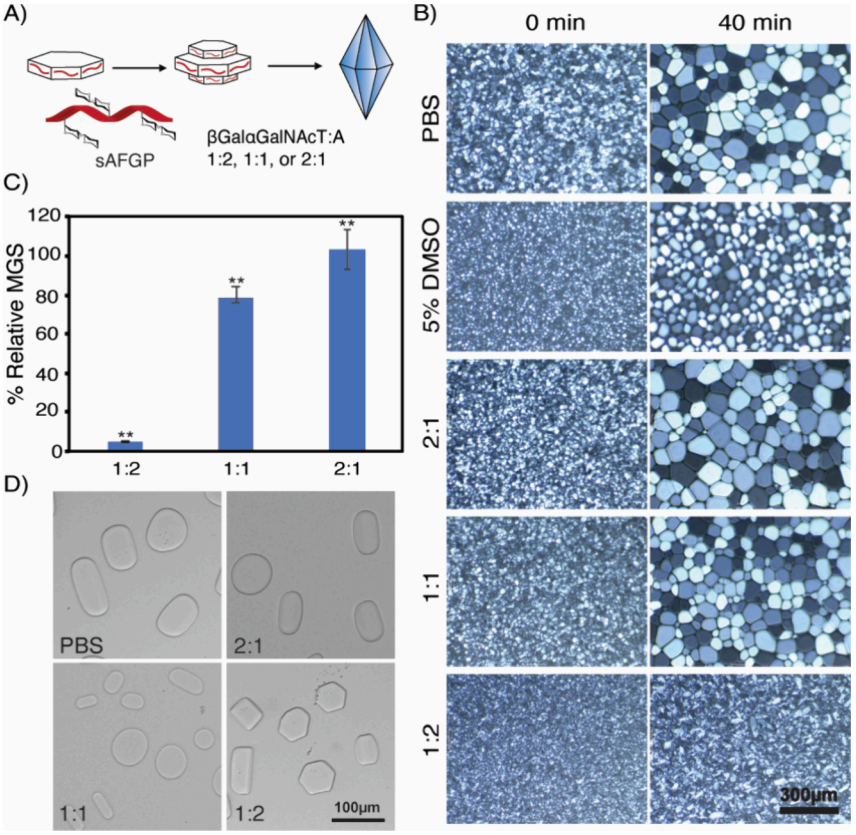

Figure 3. Ice binding properties of sAFGPs with varying amino acid compositions. (A) Cartoon illustration of ice binding and shaping in the presence of sAFGPs composed of 1:2, 1:1, or 2:1 βGalαGalNAcThr:Ala ca. 50mers. (B) Images of cooling splat assays and IRI activity for 71 μM sAFGP or 5 wt % DMSO in PBS or PBS alone. (C) Quantified IRI data as % MGS relative to PBS; mean and standard deviation, ** indicates $p < 0.01$. (D) Ice-shaping experiments with 71 μM sAFGP in PBS.

minimum at 223 nm), observed in multiple batches and spectral runs. PolyAla is a known α-helix former,[77] so we hypothesize that larger MWs may facilitate Ala-rich microdomains, though it is surprising that the 32 additional residues could have this effect. However, compared to PPII, α-helical conformations have higher intensity absorbances at identical protein concentrations and therefore could be of low relative abundance. In any case, the antifreeze activity was not affected (vide infra). Overall, we found that low MW sAFGPs are far less ordered than high MW AFGPs, correlating well with the observations of native AFGPs.

Glycan identity and density also play roles in the sAFGP conformation. Increasing βGalαGalNAcThr content while decreasing Ala led to proportional increases in extended PPII structure (maxima at ∼217 nm, Figure 2C). Clearly, βGalαGalNAcThr drives the extended PPII-like conformation. Truncation to αGalNAc in native 1:2 Thr:Ala structures resulted in a reduced PPII propensity (reduced absorbance at 217 nm, Figure 2D). αGal, βGal, and βGalNAc polymers adopt predominantly disordered conformations, indicated by the absence or reduction of the 217 nm band. These data suggest that the αGalNAc group partially orients the peptide into PPII helices, which is further stabilized by βGal(1→3) glycan extension.

sAFGP Antifreeze Activity Assays. Native AFGPs bind irreversibly to embryonic ice crystals, inhibiting prism-face growth and influencing the overall shape and size. This results in a reduction in mean grain size (MGS), i.e. IRI, and shaping of single crystals into characteristic hexagonal and bipyramidal structures (Figure 3A).[5] We used cryostage microscopy and cooling splat assays to observe ice shaping and IRI activity for sAFGP ∼50mers with varied βGalαGalNAcThr:Ala ratios.[15] Our controls were PBS and common cryoprotectant dimethyl sulfoxide (DMSO).[78] Ideally, we would compare our materials side-by-side with native fish AFGPs, but there is no current commercial source.

Increasing the Ala content correlated with higher IRI activity and stronger ice-shaping properties (Figure 3B−D). Polymers with 33% Ala displayed no IRI activity and had no effect on crystal shape. Those with 50% Ala showed minor IRI activity (22% MGS reduction) but had little impact on crystal shape. By contrast, sAFGPs with native 66% Ala and 33% βGalαGalNAcThr exhibited remarkably potent IRI activity analogous to that of native AFGPs (95% MGS reduction).[5−8,47] They also displayed identical hexagon-inducing ice-shaping properties as native AFGPs.[5,6] These findings highlight the importance of Ala in the ice-binding properties of (s)AFGPs.

IRI and ice-shaping also depended upon MW. Native ratio 1:2 βGalαGalNAcThr:Ala polymers 28, 57, or 170mers exhibited IRI activity that increases with chain length (Figure 4A,B). Compared to PBS, the relative MGS reduction was 89% for sAFGP 28mer, 94% for 57mers, and 97% for 170mers. These data align with those of native AFGPs where AFGP1−5 (33.7−10.5 kDa) show higher IRI than AFGP8 (2.65 kDa).[5,14] Ice-shaping strength also increased with sAFGP chain length; 28mers resulted in amorphous, rounded crystals, while 57mers

https://doi.org/10.1021/acs.chemmater.4c00266
Chem. Mater. 2024, 36, 3424−3434

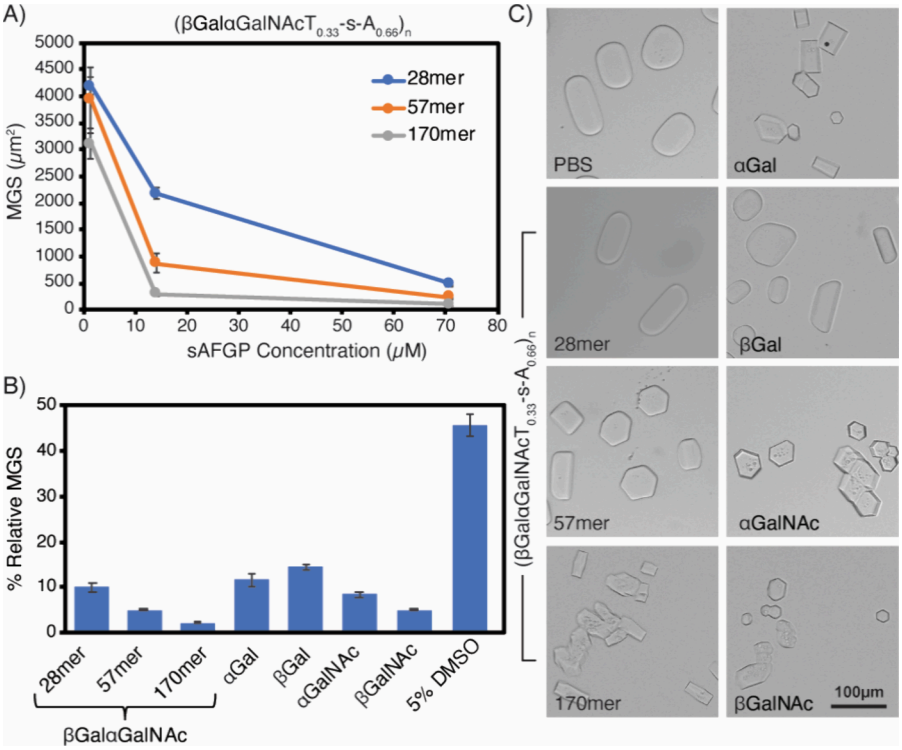

Figure 4. Ice-binding data for sAFGPs composed of the native 1:2 glycoT:A ratio and with varied chain lengths and varied glycan structures. (A) Observed absolute MGS at varied concentrations for sAFGPs with the native βGalαGalNAc disaccharide and with chain lengths of 28, 57, 170 residues. (B) Quantified IRI data as % MGS relative to PBS for native disaccharide sAFGPs of varied chain lengths as compared to sAFGP 93mers bearing monosaccharides of varied structure and anomeric linkages or 5% DMSO; sAFGP concentration is 71 μM in PBS; ice crystal MGS was determined from cooling splat assays; mean and standard deviation; table of statistical significance is in the SI. (C) Ice-shaping experiments for native disaccharide sAFGPs of varied chain lengths as compared to sAFGP 93mers bearing glycans of varied structure and anomeric linkages; sAFGP concentration is 71 μM in PBS.

and 170mers produced angular crystals with hexagonal or rectangular morphologies (Figure 4C).

Finally, we examined the ice shaping and IRI activity of sAFGPs with the native Thr:Ala ratio, moderate chain lengths (93mers), and varied glycans. All sAFGPs, regardless of the glycan identity, exhibited strong IRI activity (Figure 4B). Structures lacking NAc groups (αGal and βGal) had slightly lower activity than those with NAc (αGalNAc and βGalNAc) but remained potent antifreeze agents. Relative ice crystal MGSs from $(\alpha GalT_{0.33}\text{-}s\text{-}A_{0.66})_{93}$ and $(\beta GalT_{0.33}\text{-}s\text{-}A_{0.66})_{93}$ solutions were reduced by 88 and 85%, respectively. $(\alpha GalNAcT_{0.33}\text{-}s\text{-}A_{0.66})_{93}$ and $(\beta GalNAcT_{0.33}\text{-}s\text{-}A_{0.66})_{93}$ displayed higher activity, resulting in a relative MGS reduction of 92 and 97%. Comparing IRI activity on a mass basis yielded a similar trend (see the SI). By contrast, 5% DMSO only achieved a 54% relative reduction. In a side-by-side trial, higher PVA concentrations were required to achieve a MGS reduction similar to that of our sAFGPs (see the SI). Overall, our highest MW sAFGP of native composition, $(\beta Gal\alpha GalNAcT_{0.33}\text{-}s\text{-}A_{0.66})_{170}$, demonstrated the strongest IRI properties.

Ice-shaping patterns of glycan-variable sAFGPs aligned with IRI trends (Figure 4C). αGal- or βGal-sAFGPs resulted in a mix of rounded and rectangular crystals, while αGalNAc- and βGalNAc-sAFGPs produced predominantly ordered, angular-faced structures. Intriguingly, $(\alpha GalNAcT_{0.33}\text{-}s\text{-}A_{0.66})_{93}$ induced hexagonal crystal growth similar to native AFGPs[5,14] and our disaccharide-sAFGP. These data suggest the αGalNAcThr plays a role in sAFGP ice binding, either directly or indirectly by favorably orienting Ala or Thr methyl groups.

We speculate that the stronger activity of structures containing αGalNAc could be due to optimized peptide conformational effects driven by interaction between the sugar NAc group hydrogen bonding to the peptide backbone.[63] The disaccharide structure might have additional advantages in increased hydration sphere and water hydrogen bonding capacity compared to monosaccharides.

Our findings contradict the widely cited study by Tachibana, which claimed the α-linkage, C2 NAc, and disaccharide were all essential for antifreeze activity.[38] By contrast, our structures with mono- and disaccharides, α- and β-linkages, and with or without C2 NAc exhibit potent IRI activity. In the prior work, conclusions were drawn from structures of only ca. 6−9 amino acids that cannot adopt long-range conformations and have differing entropic considerations than macromolecular proteins. By contrast, our sAFGPs are comparable in size to native AFGPs and adopt ordered, stable extended PPII-like structures.

Interestingly, our data also indicate that while evolution has clearly optimized the tripeptide repeat and PPII-type conformation for antifreeze activity, the repeating sequence and conformation are not strictly required. Our structures with varied conformations all show high activity, indicating that the PPII conformation is not mandatory. We also conclude that because our statistical copolymers have high IRI activity, alterations in the native AAT tripeptide repeat sequence are tolerated as long as the T:A ratio remains unchanged. With the ratio of 1:2 T:A, amino acids can appear in scrambled order while maintaining IRI activity.

https://doi.org/10.1021/acs.chemmater.4c00266
Chem. Mater. 2024, 36, 3424−3434

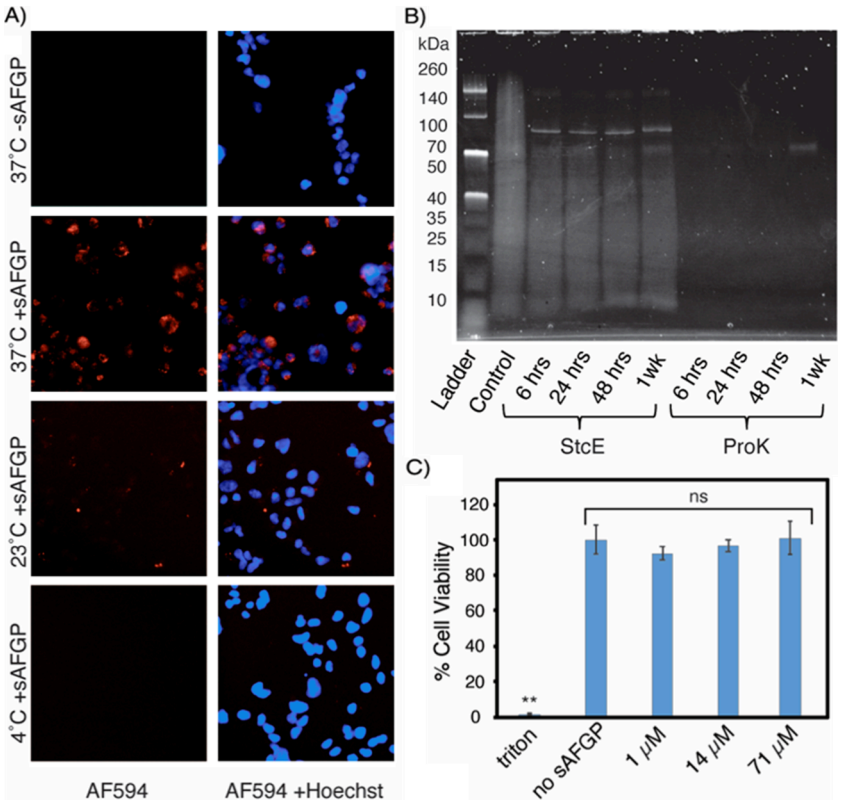

Figure 5. Cellular internalization, biodegradation, and cytocompatibility of sAFGPs with the native 1:2 glycoT:A composition and bearing the native disaccharide. (A) Internalization of sAFGP 10 μM AF594-$(\beta$GalαGalNAcT$_{0.33}$-s-A$_{0.66})_{57}$ in HEK293 cells at 4, 23, or 37 °C. (B) SDS-PAGE of protease-treated $(\beta$GalαGalNAcT$_{0.33}$-s-A$_{0.66})_{98}$ at varied time points, stained with glycoprotein-specific Pro-Q Emerald 300. (C) HEK 293 cell viability as determined by the CCK8 assay following 24 h incubation with sAFGP $(\beta$GalαGalNAcT$_{0.33}$-s-A$_{0.66})_{57}$ at the indicated concentrations; no sAFGP is media alone as a negative control and Triton X-100 was a positive control; standard deviation; ** indicates $p < 0.01$.

We did consider the possibility of the formation of short stretches of AAT repeats in our copolymers and computationally determined the probability of this explanation (see the SI). Statistical copolymers have a distribution of sequences, with residues incorporated statistically according to their unique monomer kinetics. We have previously measured kinetics of a variety of NCA monomers in this polymerization system,[49,79] including mono- and disaccharide conjugates, and while similar enough that highly tapered structures are unlikely to form, incorporation is not truly random. However, as a thought experiment, we conducted computational simulations to determine the probability of native AAT repeats occurring in random polymerizations yielding 28−170mer chains. The simulations indicate that the probability occurrence of even a single short 9-mer AAT repeat is too low to rationalize our observed data (see the SI for probability simulations and additional discussion). Therefore, we conclude that the AAT sequence is not essential so long as the relative ratios are maintained.

Our data align with previous data where short peptides with sequence-scrambled repeats showed similar activity to that of short peptides with native AAT repeats. Additionally, unlike some nonglycosylated AFPs,[80] AFGPs do not have a strict binding site and instead can interact with ice along the entire chain.[54] Considering that we show that a high Ala content is necessary for IRI activity, we reason that the activity is due to a bulk material phenomenon rather than a specific sequence. Sufficient hydrophobic contacts between polypeptide methyl groups on both Ala and Thr and the ice surface adhere the two, while solvent-oriented glycan-hydroxyls prevent ordering of approached liquid water molecules via hydrogen bonding interactions. This rationale aligns nicely with molecular simulations indicating both Ala and Thr methyl groups drive ice binding.[54] Similar works on PVA,[39,41,42] proline[40] polymers, and Ala-s-Lys copolymers[81,82] indicate that IRI activity is not necessarily dependent on a specific sequence but rather can be effected by bulk phenomenon. Overall, our data indicate that there is more flexibility in molecular design of AFGP mimic than previously thought and shed light on the debate of the role of the disaccharide, the NAc group, and the Ala residues.

Cytocompatibility, Cell Internalization, and Degradation of sAFGPs. In polar fish, AFGPs are present in the interstitial fluid of all body tissues except brain tissue, but intracellular accumulation has not been observed.[83] Surprisingly, little is known regarding the intracellular accumulation of AFGPs in the context of cryopreservation. A single report describes internalization of AFGP8 in human embryonic liver cells and trout gill cells.[84] Additionally, limited evidence suggests cell membrane interactions.[85−87] Internalization could be important in the context of cryopreservation, where intracellular accumulation could prevent intracellular ice or have downstream biological effects. Therefore, we investigated the interaction of our sAFGPs with live human cells.

We labeled $(\beta$GalαGalNAcT$_{0.33}$-s-A$_{0.66})_{57}$ with AF594 using *N*-hydroxysuccinimide ester chemistry. We investigated internalization in human red blood cells (hRBCs), white blood cells (Raji), and embryonic kidney cells (HEK293), representing suspension and adherent models of either

https://doi.org/10.1021/acs.chemmater.4c00266
Chem. Mater. 2024, 36, 3424−3434

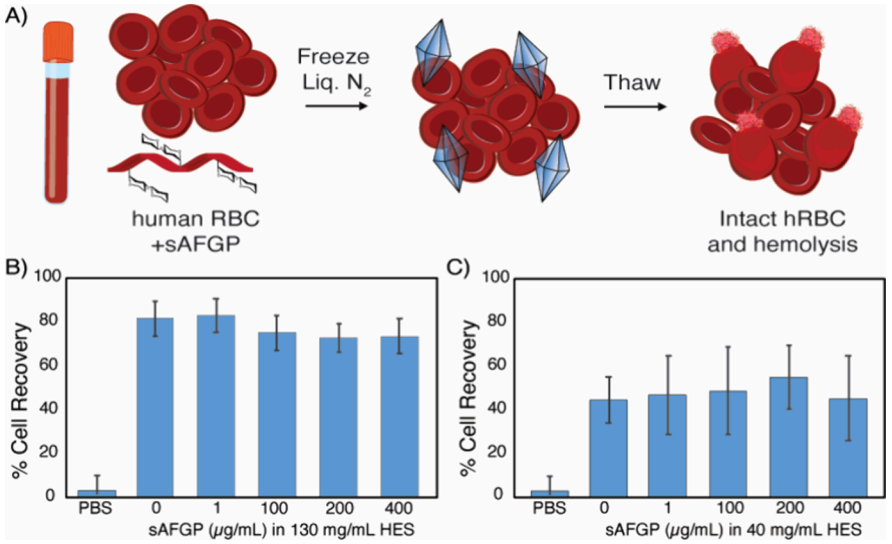

Figure 6. Cryopreservation of hRBCs in sAFGP supplemented HES solutions or PBS alone. (A) Schematic representation of the hRBC cryopreservation experimental workflow and cell hemolysis as the assessment metric of cell survival. (B, C) Post-thaw intact hRBC cell recovery by hemolysis assays after freezing with sAFGP (βGalαGalNAcT$_{0.33}$-*s*-A$_{0.66}$)$_{170}$ and (B) 130 mg/mL HES or (C) 40 mg/mL HES. Data are the result of two separate experiments performed in triplicate. Within each experiment, the cell recovery is not statistically different across the varied treatments.

therapeutic value or to benchmark against the previous AFGP8 study. Following a 1 h incubation with sAFGP-594 at 37 °C, we observed substantial internalization and distribution within Raji and HEK cells but not within hRBCs (Figure 5A and SI). As hRBCs do not normally endocytose,[88] this potentially suggests an endocytic uptake mechanism rather than passive translocation. Additionally, we examined uptake at endocytosis-inhibiting temperatures (4 and 23 °C), and minimal sAFGP was internalized (Figure 5A). Quantification of polymer internalization can be found in the SI and additional work is underway to probe this phenomenon.

Considering that (s)AFGPs can be internalized into cells, we investigated their potential for protease degradation. In the context of biomedical applications, such as cryopreservation, intracellular accumulation with no degradation pathway is typically undesirable. We treated moderately sized sAFGP (βGalαGalNAcT$_{0.33}$-*s*-A$_{0.66}$)$_{98}$ with nonspecific proteinase K (ProK), which cleaves preferentially after hydrophobic sites,[89] and glycoprotease secreted protease of C1 esterase (StcE), which cleaves before αGalNAc-Ser/Thr.[90] ProK efficiently degraded the sAFGP within 6 h, while StcE only partially degraded the sample over 1 week (Figure 5B); likely, StcE prefers a monosaccharide substrate. It should be noted that the broad bands were expected since the sAFGPs are heavily glycosylated and neutral and, therefore, do not interact strongly with SDS. Broad bands are quite typical for native fish AFGPs and structurally related mucins.[57,91] Overall, sAFGPs are unlikely to bioaccumulate.

Toxic effects were unexpected since native AFGPs are present at up to 25 mg/mL in fish blood[1] and similar synthetic glycopolypeptides are nontoxic.[92] Considering their validated internalization behavior, we assessed (βGalαGalNAcT$_{0.33}$-*s*-A$_{0.66}$)$_{57}$ with HEK293 cells. CCK8 assays were conducted after 24 h at 37 °C with sAFGP concentrations relevant to IRI. At the highest concentration tested, there were no statistically significant effects on cellular viability (Figure 5C). Prior to cryopreservation, cells are typically suspended and growth media and exchanged for freezing media containing suitable cryoprotectant agents. Exposure to cryoprotectants is typically quick and at reduced temperatures as the media exchange is conducted immediately prior to cell freezing. Therefore, since the conditions that we explored were far more stringent than this with no ill effects observed, we conclude that these materials are suitable for cryopreservation applications.

sAFGPs as Cellular Cryoprotectants. Cryopreservation is crucial for preserving cells and tissues for regenerative medicine and research but requires use of cryoprotective agents (CPAs) to prevent ice crystal formation and cell damage.[12,13] Little has changed in over 70 years,[93] and DMSO and glycerol are standard CPAs despite well-known toxic effects.[78,94] Hydroxyethyl starch (HES) is a newer better-tolerated CPA, favorable due to membrane-impermanence, but still has associated toxic effects.[95] Plus, excessive solution viscosity presents processing challenges. AFGPs have the potential to revolutionize biomedical cryopreservation by replacing or reducing toxic CPAs. However, conflicting results and a lack of consensus on optimal cryopreservation conditions hinder their widespread use.[96,97]

For an initial study, we benchmarked our sAFGPs against a report utilizing native AFGPs combined with HES to freeze hRBCs.[85] In their study, flash-freezing in liquid nitrogen with 130 mg/mL HES and slow thawing at ∼20 °C resulted in 12% cell survival. Addition of 1−800 μg/mL AFGP1−5 increased cell recovery up to 24% but did not scale linearly and was optimized at 200 μg/mL. In our hands, hemolysis assays after flash-freezing of hRBCs with 130 mg/mL HES and 0−400 μg/mL (βGalαGalNAcT$_{0.33}$-*s*-A$_{0.66}$)$_{170}$ followed by slow thaw at 23 °C resulted in 3% cell recovery for PBS and 80% for HES alone, which hindered observation of any sAFGP effects (Figure 6A, B). Therefore, we assessed hRBC hemolysis at varied HES concentrations and identified 40 mg/mL as having 20% post-thaw viability (see the SI). Freeze−thaw experiments with 40 mg/mL HES supplemented with 0−400 μg/mL sAFGP showed no statistically significant effect of the sAFGPs on hRBC survival. Similar results were obtained for HEK293 cells (see the SI).

This result was not surprising, considering the modest effects of the native AFGP-HES combination in the prior study. In

https://doi.org/10.1021/acs.chemmater.4c00266
Chem. Mater. 2024, 36, 3424−3434

fact, in their work, freeze−thaw with AFGPs alone actually decreased cell survival compared to PBS alone. Differences in our studies could be due to HES molecular weight or functionalization degree, which were not reported, varying thaw methodology, or the heterogeneity of native AFGPs and their challenging purification. Given the potent IRI and ice-shaping activity of the sAFGPs, which are comparable to native AFGPs, further research on freezing methodology and CPA combinations is warranted and is underway.

CONCLUSIONS

AFGPs have diverse applications in agriculture, food, surface coatings, and biomedical tissue cryopreservation. However, their isolation from polar organisms is cumbersome and impractical, hindering research on these unique molecules and their mechanisms of action. Here, we present a rapid and scalable method for synthetic AFGPs, allowing facile customization of molar mass and amino acid and glycan composition. We investigated a range of structures and found that hydrophobic Ala is essential for antifreeze activity, and potency increases with molecular weight. While the native disaccharide displayed the highest potency, all glycan structures examined exhibited IRI properties. These polymers are active at concentrations far lower than those of previously reported synthetic antifreeze polymers. Our synthetic AFGPs are internalized by human cell lines, nontoxic, and biodegradable but did not alter red blood cell cryopreservation outcomes when used in combination with HES. In ice-binding studies, the synthetic AFGPs performed essentially identically to native AFGPs, indicating their promise as surrogates for these elusive natural structures.

METHODS

General Method for Polymerization of NCAs. All polymerizations were prepared in a N_2-filled glovebox. NCAs were dissolved in anhydrous THF at 50 mg/mL in a glass vial or a bomb tube. To the NCA solution, a 30 mg/mL solution of $(PMe_3)_4Co$ in THF was added and the tube was sealed. The NCA:$(PMe_3)_4Co$ ratio ranged from 10:1 to 80:1, yielding different length polypeptides. The vials were left in the glovebox at RT and the bomb tubes were removed from the glovebox and heated at 50 °C for 5−72 h. The reaction progress was monitored by attenuated total reflectance-Fourier transform infrared spectroscopy (ATR-FTIR). Upon completion, the polypeptides were analyzed with SEC/MALS/RI.

General Method for Polymerization of Statistical Copolymers. Copolymers were prepared in a N_2 filled glovebox in a manner similar to that for homopolymers. The NCAs were dissolved in THF at 50 mg/mL and mixed at a variety of NCA molar ratios. $(PMe_3)_4Co$ catalyst in THF (30 mg/mL) was added to the combined NCA solutions, and the reaction progressed at RT and was monitored by ATR-FTIR. Polypeptides that remained soluble were analyzed using SEC/MALS/RI.

General Method for Observing Dynamic Ice Shaping. A 10 μL solution containing sAFGP in 1× PBS was placed on a microscope slide and sandwiched between a coverslip. The stage was rapidly cooled at a rate of 10 °C/min to −30 °C to freeze the solution. The stage was then slowly warmed to −2.5 °C at a rate of 8 °C/min. Then, the stage was warmed to −1.8 °C at a rate of 0.5 °C/min. The stage temperature was then increased at a rate of 0.05 °C/min to −1.5 to −1 °C depending on the polypeptide solution to isolate individual crystals. The stage was then cooled at 0.02 °C/min to −2 to −1.5 °C to observe dynamic ice shaping. The stage was then toggled between melting and freezing rates to observe the ice crystal change as the temperature was increased and then decreased. Images of the single crystals were taken as the temperature was decreased to observe ice crystal growth.

General Method for Cooling Splat Assays. Using a micropipette, 10 μL of sAFGP in PBS was dropped from 2 m through a PVC pipe onto a precooled glass slide (aluminum block resting in a bed of dry ice) at −78.5 °C to form a thin wafer. The slide containing the ice splat was quickly moved to a temperature-controlled microscope stage (Linkam LTS120, WCP, and T96 controller) precooled to −6.4 °C. See SI Notes 1−3 for details. Typically, ice wafers are annealed at a temperature ranging from −6 to 8 °C to ensure that a eutectic phase is present at the crystal boundary and the ice is able to undergo recrystallization.[98,99] Use of PBS or a saline solution is essential due to the overestimation of IRI activity if observed in pure water.[98,99] The ice wafers were annealed for 40 min at −6.4 °C, and images of the ice crystals were recorded at 0, 20, and 40 min using cross polarizers (MOTICAM S3, MOTIC BA310E LED Trinocular) to observe ice recrystallization inhibition. The stage chamber was purged with N_2 to prevent condensation from growing on the ice splat (see SI Note 4). From the images, ice MGS was determined by using image processing software or manual measurements. To ensure statistical significance, three images were obtained for each sample, and grain sizes within a minimum of three 150 μm^2 regions per sample were measured. Regions toward the center of the wafer rather than near the edges were selected.

General Method for Glycopolypeptide Cellular Internalization Studies with HEK293 Cells. HEK 293 cells were plated on three 24-well plates and incubated at 37 °C in 5% CO_2 overnight to allow the cells to adhere. After 24 h, the cell media were removed. A 100 μM solution of A594-$(\beta Gal\alpha GalNAcT_{0.33}\text{-}s\text{-}A_{0.66})_{57}$ in Milli-Q was diluted in complete media to make a 10 μM solution of polypeptide. The solution was sterile-filtered before 300 μL of the solution was applied to the cells. Additionally, 300 μL of complete medium was applied to additional wells of cells to serve as the untreated control. The 24-well plates were then placed at 37 °C, RT (23 °C), and 4 °C to incubate for 1 h. After 1 h, the media were removed and the cells were rinsed 3× with DPBS. A 500 μL amount of Hoescht stain was then added to each well, and cells were incubated for 10 min at RT. The cells were then fluorescently imaged to observe the localization of the fluorescent polymer.

General Method for Freezing and Thawing hRBCs for Cryoprotection Studies. The cryopreservation of hRBC was conducted following published procedures.[85] In short, 50 μL of hRBCs (prepared as discussed in the SI) were mixed with 50 μL of DPBS containing cryoprotectants or control solution in cryovials. The vials were then placed in a liquid nitrogen bath for 20 min. The samples were then thawed at room temperature for 20 min. Control samples were also prepared according to this publication. hRBCs were added to water and frozen for 100% hemolysis, and for 0% hemolysis, hRBCs were incubated with DPBS at room temperature for 1 h. For all hRBC cryopreservation experiments, 2-hydroxyethyl starch (Spectrum Chemical, H3012) was used.

ASSOCIATED CONTENT

Supporting Information

The Supporting Information is available free of charge at https://pubs.acs.org/doi/10.1021/acs.chemmater.4c00266.

Full experimental details, characterization of compounds, instrumentation, complete IRI and ice shaping images, computational simulation data, and additional figures and data (PDF)

AUTHOR INFORMATION

Corresponding Author

Jessica R. Kramer − *Department of Biomedical Engineering, University of Utah, Salt Lake City, Utah 84112, United States;* orcid.org/0000-0002-4268-0126; Email: jessica.kramer@utah.edu

https://doi.org/10.1021/acs.chemmater.4c00266
Chem. Mater. 2024, 36, 3424−3434

Authors

Anna C. Deleray − *Department of Biomedical Engineering, University of Utah, Salt Lake City, Utah 84112, United States;* orcid.org/0000-0002-2191-3058

Simranpreet S. Saini − *Department of Biomedical Engineering, University of Utah, Salt Lake City, Utah 84112, United States*

Alexander C. Wallberg − *Department of Biomedical Engineering, University of Utah, Salt Lake City, Utah 84112, United States*

Complete contact information is available at: https://pubs.acs.org/10.1021/acs.chemmater.4c00266

Author Contributions

The manuscript was written through contributions of all authors. All authors have given approval to the final version of the manuscript.

Funding

Prof. Jessica Kramer acknowledges financial support from USA NIH NIGMS 1R35GM147262-01, USA NSF DMR-1848054, and DMR-2300012.

Notes

The authors declare no competing financial interest.

■ ACKNOWLEDGMENTS

We acknowledge the lab of Prof. Michael Yu, Department of Biomedical Engineering, University of Utah, for the use of their CD spectrometer and the lab of Prof. Russell Stewart and Monika Sima for use of their aqueous SEC/MALS/RI. We thank Guanqun Ma, Scientific Computing and Imaging Institute (SCI Institute), University of Utah, for assistance with probability simulations.

■ REFERENCES

(1) DeVries, A. L.; Wohlschlag, D. E. Freezing Resistance in Some Antarctic Fishes. *Science (80-.).* **1969**, *163*, 1073−1075.

(2) Scholander, P. F.; van Dam, L.; Kanwisher, J. W.; Hammel, H. T.; Gordon, M. S. Supercooling and osmoregulation in arctic fish. *J. Cell. Comp. Physiol.* **1957**, *49*, 5−24.

(3) Gordon, M. S.; Amdur, B. H.; Scholander, P. F. Freezing Resistance in Some Northern Fishes. *Biol. Bull.* **1962**, *122*, 52−62.

(4) Graham, L. A.; Davies, P. L. Glycine-Rich Antifreeze Proteins from Snow Fleas. *Science (80-.).* **2005**, *310*, 461−461.

(5) Meister, K.; Devries, A. L.; Bakker, H. J.; Drori, R. Antifreeze Glycoproteins Bind Irreversibly to Ice. *J. Am. Chem. Soc.* **2018**, *140*, 9365−9368.

(6) Berger, T.; et al. Synergy between Antifreeze Proteins Is Driven by Complementary Ice-Binding. *J. Am. Chem. Soc.* **2019**, *141*, 19144−19150.

(7) DeVries, A. L.; Komatsu, S. K.; Feeney, R. E. Chemical and physical properties of freezing point-depressing glycoproteins from Antarctic fishes. *J. Biol. Chem.* **1970**, *245*, 2901−2908.

(8) DeVries, A. L. Glycoproteins as biological antifreeze agents in Antarctic fishes. *Science (80-.).* **1971**, *172*, 1152−1155.

(9) Eskandari, A.; Leow, T. C.; Rahman, M. B. A.; Oslan, S. N. Antifreeze proteins and their practical utilization in industry, medicine, and agriculture. *Biomolecules* **2020**, *10*, 1−18.

(10) Voets, I. K. From ice-binding proteins to bio-inspired antifreeze materials. *Soft Matter* **2017**, *13*, 4808−4823.

(11) Meldolesi, A. GM fish ice cream. *Nat. Biotechnol.* **2009**, *27*, 682−682.

(12) Bojic, S.; et al. Winter is coming: the future of cryopreservation. *BMC Biol.* **2021**, *19*, 56.

(13) Brockbank, K. G. M.; Campbell, L. H.; Greene, E. D.; Brockbank, M. C. G.; Duman, J. G. Lessons from nature for preservation of mammalian cells, tissues, and organs. *Vitr. Cell. Dev. Biol. - Anim.* **2011**, *47*, 210−217.

(14) Budke, C.; et al. Quantitative efficacy classification of ice recrystallization inhibition agents. *Cryst. Growth Des.* **2014**, *14*, 4285−4294.

(15) Knight, C. A.; De Vries, A. L.; Oolman, L. D. Fish antifreeze protein and the freezing and recrystallization of ice. *Nature* **1984**, *308*, 295−296.

(16) Chen, L.; Devries, A. L.; Cheng, C. H. C. Convergent evolution of antifreeze glycoproteins in Antarctic notothenioid fish and Arctic cod. *Proc. Natl. Acad. Sci. U. S. A.* **1997**, *94*, 3817−3822.

(17) Giubertoni, G.; Meister, K.; DeVries, A. L.; Bakker, H. J. Determination of the Solution Structure of Antifreeze Glycoproteins Using Two-Dimensional Infrared Spectroscopy. *J. Phys. Chem. Lett.* **2019**, *10*, 352−357.

(18) Urbańczyk, M.; Góra, J.; Latajka, R.; Sewald, N. Antifreeze glycopeptides: from structure and activity studies to current approaches in chemical synthesis. *Amino Acids* **2017**, *49*, 209−222.

(19) Naullage, P. M.; Metya, A. K.; Molinero, V. Computationally efficient approach for the identification of ice-binding surfaces and how they bind ice. *J. Chem. Phys.* **2020**, *153*, No. 174106.

(20) Her, C.; Yeh, Y.; Krishnan, V. V. The ensemble of conformations of antifreeze glycoproteins (AFGP8): A study using nuclear magnetic resonance spectroscopy. *Biomolecules* **2019**, *9*, 235.

(21) Raymond, J. A.; Radding, W.; DeVries, A. L. Circular dichroism of protein and glycoprotein fish antifreezes. *Biopolymers* **1977**, *16*, 2575−2578.

(22) Franks, F.; Morris, E. R. Blood glycoprotein from antarctic fish possible conformational origin of antifreeze activity. *Biochim. Biophys. Acta - Gen. Subj.* **1978**, *540*, 346−356.

(23) Detwiler, R. E.; Schlirf, A. E.; Kramer, J. R. Rethinking Transition Metal Catalyzed N-Carboxyanhydride Polymerization: Polymerization of Pro and AcOPro N-Carboxyanhydrides. *J. Am. Chem. Soc.* **2021**, *143*, 11482−11489.

(24) Carvajal-Rondanelli, P. A.; Marshall, S. H.; Guzman, F. Antifreeze glycoprotein agents: Structural requirements for activity. *J. Sci. Food Agric.* **2011**, *91*, 2507−2510.

(25) DeVries, A. L. Antifreeze glycopeptides and peptides: Interactions with ice and water. *Methods Enzymol.* **1986**, *127*, 293−303.

(26) Biggs, C. I.; et al. Polymer mimics of biomacromolecular antifreezes. *Nat. Commun.* **2017**, *8*, 1546.

(27) Tachibana, Y.; et al. Efficient and versatile synthesis of mucin-like glycoprotein mimics. *Tetrahedron* **2002**, *58*, 10213−10224.

(28) Wilkinson, B. L.; et al. Total synthesis of homogeneous antifreeze glycopeptides and glycoproteins. *Angew. Chemie - Int. Ed.* **2012**, *51*, 3606−3610.

(29) Eniade, A.; Murphy, A. V.; Landreau, G.; Ben, R. N. A general synthesis of structurally diverse building blocks for preparing analogues of C-linked antifreeze glycoproteins. *Bioconjugate Chem.* **2001**, *12*, 817−823.

(30) Tseng, P. H.; Jiaang, W. T.; Chang, M. Y.; Chen, S. T. Facile solid-phase synthesis of an antifreeze glycoprotein. *Chem. - A Eur. J.* **2001**, *7*, 585−590.

(31) Eniade, A.; Ben, R. N. Fully convergent solid phase synthesis of antifreeze glycoprotein analogues. *Biomacromolecules* **2001**, *2*, 557−561.

(32) Graham, B.; et al. Polyproline as a Minimal Antifreeze Protein Mimic That Enhances the Cryopreservation of Cell Monolayers. *Angew. Chem.* **2017**, *56*, 15941−15944.

(33) Ben, R. N.; Eniade, A. A.; Hauer, L. Synthesis of a C-linked antifreeze glycoprotein (AFGP) mimic: Probes for investigating the mechanism of action. *Org. Lett.* **1999**, *1*, 1759−1762.

(34) Liu, S.; Ben, R. N. C-linked galactosyl serine AFGP analogues as potent recrystallization inhibitors. *Org. Lett.* **2005**, *7*, 2385−2388.

(35) Tsuda, T.; Nishimura, S. I. Synthesis of an antifreeze glycoprotein analogue: Efficient preparation of sequential glycopeptide polymers. *Chem. Commun.* **1996**, 2779−2780.

(36) Huang, M. L.; et al. Biomimetic peptoid oligomers as dual-action antifreeze agents. *Proc. Natl. Acad. Sci. U. S. A.* **2012**, *109*, 19922−19927.
(37) Filira, F.; et al. Solid phase synthesis and conformation of sequential glycosylated polytripeptide sequences related to antifreeze glycoproteins. *Int. J. Biol. Macromol.* **1990**, *12*, 41−49.
(38) Tachibana, Y.; et al. Antifreeze glycoproteins: Elucidation of the structural motifs that are essential for antifreeze activity. *Angew. Chemie - Int. Ed.* **2004**, *43*, 856−862.
(39) Deller, R. C.; Vatish, M.; Mitchell, D. A.; Gibson, M. I. Synthetic polymers enable non-vitreous cellular cryopreservation by reducing ice crystal growth during thawing. *Nat. Commun.* **2014**, *5*, 3244.
(40) Judge, N.; et al. High Molecular Weight Polyproline as a Potential Biosourced Ice Growth Inhibitor: Synthesis, Ice Recrystallization Inhibition, and Specific Ice Face Binding. *Biomacromolecules* **2023**, *24*, 2459−2468.
(41) Tekin, K.; Daşkın, A. Effect of polyvinyl alcohol on survival and function of angora buck spermatozoa following cryopreservation. *Cryobiology* **2019**, *89*, 60−67.
(42) Six, K. R.; Lyssens, S.; Devloo, R.; Compernolle, V.; Feys, H. B. The ice recrystallization inhibitor polyvinyl alcohol does not improve platelet cryopreservation. *Transfusion* **2019**, *59*, 3029−3031.
(43) Graham, B.; Fayter, A. E. R.; Houston, J. E.; Evans, R. C.; Gibson, M. I. Facially Amphipathic Glycopolymers Inhibit Ice Recrystallization. *J. Am. Chem. Soc.* **2018**, *140*, 5682−5685.
(44) Mitchell, D. E.; Cameron, N. R.; Gibson, M. I. Rational, yet simple, design and synthesis of an antifreeze-protein inspired polymer for cellular cryopreservation. *Chem. Commun.* **2015**, *51*, 12977−12980.
(45) Gibson, M. I.; Barker, C. A.; Spain, S. G.; Albertin, L.; Cameron, N. R. Inhibition of ice crystal growth by synthetic glycopolymers: Implications for the rational design of antifreeze glycoprotein mimics. *Biomacromolecules* **2009**, *10*, 328−333.
(46) Acker, J. P.; et al. Small molecule ice recrystallization inhibitors enable freezing of human red blood cells with reduced glycerol concentrations. *Transfus. Med. Rev.* **2015**, *29*, 277.
(47) Balcerzak, A. K.; Capicciotti, C. J.; Briard, J. G.; Ben, R. N. Designing ice recrystallization inhibitors: from antifreeze (glyco)-proteins to small molecules. *RSC Adv.* **2014**, *4*, 42682−42696.
(48) Campos-García, V. R.; et al. Process signatures in glatiramer acetate synthesis: Structural and functional relationships. *Sci. Rep.* **2017**, *7*, 1−12.
(49) Kramer, J. R.; Onoa, B.; Bustamante, C.; Bertozzi, C. R. Chemically tunable mucin chimeras assembled on living cells. *Proc. Natl. Acad. Sci. U. S. A.* **2015**, *112*, 12574−12579.
(50) Deleray, A. C.; Kramer, J. R. Biomimetic Glycosylated Polythreonines by N-Carboxyanhydride Polymerization. *Biomacromolecules* **2022**, *23*, 1453−1461.
(51) Raymond, J. A.; DeVries, A. L. Adsorption inhibition as a mechanism of freezing resistance in polar fishes. *Proc. Natl. Acad. Sci. U. S. A.* **1977**, *74*, 2589−2593.
(52) Liu, K.; et al. Janus effect of antifreeze proteins on ice nucleation. *Proc. Natl. Acad. Sci. U. S. A.* **2016**, *113*, 14739−14744.
(53) Ben, R. N. Antifreeze glycoproteins - Preventing the growth of ice. *ChemBioChem.* **2001**, *2*, 161−166.
(54) Mochizuki, K.; Molinero, V. Antifreeze Glycoproteins Bind Reversibly to Ice via Hydrophobic Groups. *J. Am. Chem. Soc.* **2018**, *140*, 4803−4811.
(55) Pandey, P.; Mallajosyula, S. S. Elucidating the role of key structural motifs in antifreeze glycoproteins. *Phys. Chem. Chem. Phys.* **2019**, *21*, 3903−3917.
(56) Ebbinghaus, S.; et al. Antifreeze glycoprotein activity correlates with long-range protein-water dynamics. *J. Am. Chem. Soc.* **2010**, *132*, 12210−12211.
(57) Tsuda, S.; et al. Fish-derived antifreeze proteins and antifreeze glycoprotein exhibit a different ice-binding property with increasing concentration. *Biomolecules* **2020**, *10*, 423.
(58) Sarno, D. M.; Murphy, A. V.; DiVirgilio, E. S.; Jones, W. E.; Ben, R. N. Direct observation of antifreeze glycoprotein-fraction 8 on hydrophobic and hydrophilic interfaces using atomic force microscopy. *Langmuir* **2003**, *19*, 4740−4744.
(59) Younes-Metzler, O.; Ben, R. N.; Giorgi, J. B. The adsorption of antifreeze glycoprotein fraction 8 on dry and wet mica. *Colloids Surfaces B Biointerfaces* **2011**, *82*, 134−140.
(60) Hederos, M.; Konradsson, P.; Borgh, A.; Liedberg, B. Mimicking the properties of antifreeze glycoproteins: Synthesis and characterization of a model system for ice nucleation and antifreeze studies. *J. Phys. Chem. B* **2005**, *109*, 15849−15859.
(61) Shier, W. T.; Lin, Y.; De Vries, A. L. Structure and mode of action of glycoproteins from an antarctic fish. *BBA - Protein Struct.* **1972**, *263*, 406−413.
(62) Sun, Y.; et al. Disaccharide Residues are Required for Native Antifreeze Glycoprotein Activity. *Biomacromolecules* **2021**, *22*, 2595−2603.
(63) Coltart, D. M.; et al. Principles of mucin architecture: Structural studies on synthetic glycopeptides bearing clustered mono-, di-, tri-, and hexasaccharide glycodomains. *J. Am. Chem. Soc.* **2002**, *124*, 9833−9844.
(64) Mimura, Y.; Yamamoto, Y.; Inoue, Y.; Chûjô, R. N.m.r. study of interaction between sugar and peptide moieties in mucin-type model glycopeptides. *Int. J. Biol. Macromol.* **1992**, *14*, 242−248.
(65) Lambu, M. R.; et al. Synthesis of C-spiro-glycoconjugates from sugar lactones via zinc mediated Barbier reaction. *RSC Adv.* **2014**, *4*, 11023−11028.
(66) Kramer, J. R.; Deming, T. J. General method for purification of α-amino acid-N-carboxyanhydrides using flash chromatography. *Biomacromolecules* **2010**, *11*, 3668−3672.
(67) Deming, T. J.; Curtin, S. A. Chain initiation efficiency in cobalt- and nickel-mediated polypeptide synthesis. *J. Am. Chem. Soc.* **2000**, *122*, 5710−5717.
(68) Deming, T. J. Cobalt and iron initiators for the controlled polymerization of α-amino acid-N-carboxyanhydrides. *Macromolecules* **1999**, *32*, 4500−4502.
(69) Cheng, J.; Deming, T. J. Synthesis of polypeptides by ring-opening polymerization of α-Amino acid N-carboxyanhydrides. *Top. Curr. Chem.* **2011**, *310*, 1.
(70) Curtin, S. A.; Deming, T. J. Initiators for end-group functionalized polypeptides via tandem addition reactions. *J. Am. Chem. Soc.* **1999**, *121*, 7427−7428.
(71) Brzezinska, K. R.; Curtin, S. A.; Deming, T. J. Polypeptide end-capping using functionalized isocyanates: Preparation of pentablock copolymers. *Macromolecules* **2002**, *35*, 2970−2976.
(72) van Stokkum, I. H.; Spoelder, H. J.; Bloemendal, M.; van Grondelle, R.; Groen, F. C. Estimation of protein secondary structure and error analysis from circular dichroism spectra. *Anal. Biochem.* **1990**, *191*, 110−118.
(73) Provencher, S. W.; Glöckner, J. Estimation of Globular Protein Secondary Structure from Circular Dichroism. *Biochemistry* **1981**, *20*, 33−37.
(74) Chemes, L. B.; Alonso, L. G.; Noval, M. G.; De Prat-Gay, G. Circular dichroism techniques for the analysis of intrinsically disordered proteins and domains. *Methods Mol. Biol.* **2012**, *895*, 387−404.
(75) Lopes, J. L. S.; Miles, A. J.; Whitmore, L.; Wallace, B. A. Distinct circular dichroism spectroscopic signatures of polyproline II and unordered secondary structures: Applications in secondary structure analyses. *Protein Sci.* **2014**, *23*, 1765−1772.
(76) Detwiler, R. E.; McPartlon, T. J.; Coffey, C. S.; Kramer, J. R. Clickable Polyprolines from Azido-proline N -Carboxyanhydride. *ACS Polym. Au* **2023**, *3*, 383−393.
(77) Yang, J.; Zhao, K.; Gong, Y.; Vologodskii, A.; Kallenbach, N. R. α-Helix nucleation constant in copolypeptides of alanine and ornithine or lysine. *J. Am. Chem. Soc.* **1998**, *120*, 10646−10652.
(78) Best, B. P. Cryoprotectant Toxicity: Facts, Issues, and Questions. *Rejuvenation Res.* **2015**, *18*, 422−436.

(79) Clauss, Z. S.; et al. Tunable, biodegradable grafting-from glycopolypeptide bottlebrush polymers. *Nat. Commun.* **2021**, *12*, 6472.
(80) Garnham, C. P.; et al. Compound ice-binding site of an antifreeze protein revealed by mutagenesis and fluorescent tagging. *Biochemistry* **2010**, *49*, 9063−9071.
(81) Park, S.; Piao, Z.; Park, J. K.; Lee, H. J.; Jeong, B. Ice Recrystallization Inhibition Using l -Alanine/ l -Lysine Copolymers. *ACS Appl. Polym. Mater.* **2022**, *4*, 2896−2907.
(82) Piao, Z.; Park, J. K.; Patel, M.; Lee, H. J.; Jeong, B. Poly(L-Ala-co-L-Lys) Exhibits Excellent Ice Recrystallization Inhibition Activity. *ACS Macro Lett.* **2021**, *10*, 1436−1442.
(83) Ahlgren, J. A.; Cheng, C. C.; Schrag, J. D.; DeVries, A. L. Freezing avoidance and the distribution of antifreeze glycopeptides in body fluids and tissues of Antarctic fish. *J. Exp. Biol.* **1988**, *137*, 549−563.
(84) Lui, S.; et al. In vitro studies of antifreeze glycoprotein (AFGP) and a C-linked AFGP analogue. *Biomacromolecules* **2007**, *8*, 1456−1462.
(85) Sun, Y.; et al. Ice Recrystallization Inhibition Is Insufficient to Explain Cryopreservation Abilities of Antifreeze Proteins. *Biomacromolecules* **2022**, *23*, 1214−1220.
(86) Wu, Y.; Banoub, J.; Goddard, S. V.; Kao, M. H.; Fletcher, G. L. Antifreeze glycoproteins: Relationship between molecular weight, thermal hysteresis and the inhibition of leakage from liposomes during thermotropic phase transition. *Comp. Biochem. Physiol. - B Biochem. Mol. Biol.* **2001**, *128*, 265−273.
(87) Hays, L. M.; Feeney, R. E.; Crowe, L. M.; Crowe, J. H.; Oliver, A. E. Antifreeze glycoproteins inhibit leakage from liposomes during thermotropic phase transitions. *Proc. Natl. Acad. Sci. U. S. A.* **1996**, *93*, 6835−6840.
(88) Schekman, R.; Singer, S. J. Clustering and endocytosis of membrane receptors can be induced in mature erythrocytes of neonatal but not adult humans. *Proc. Natl. Acad. Sci. U. S. A.* **1976**, *73*, 4075−4079.
(89) Rawlings, N. D.; Barrett, A. J.; Rawlings, N. D.; Barrett, A. J. *Handbook of Proteolytic Enzymes* Handb. Proteolytic Enzym. 1−3, *3*, 2013 Academic Press DOI: DOI: 10.1016/B978-0-12-382219-2.00001-6.
(90) Malaker, S. A.; et al. The mucin-selective protease StcE enables molecular and functional analysis of human cancer-associated mucins. *Proc. Natl. Acad. Sci. U. S. A.* **2019**, *116*, 7278−7287.
(91) Pan, H.; Colville, M. J.; Supekar, N. T.; Azadi, P.; Paszek, M. J. Sequence-Specific Mucins for Glycocalyx Engineering. *ACS Synth. Biol.* **2019**, *8*, 2315−2326.
(92) Wardzala, C. L.; Clauss, Z. S.; Kramer, J. R. Principles of glycocalyx engineering with hydrophobic-anchored synthetic mucins. *Front. Cell Dev. Biol.* **2022**, *10*, 1−13.
(93) Lovelock, J. E.; Bishop, M. W. H. Prevention of freezing damage to living cells by dimethyl sulfoxide. *Nature* **1959**, *183*, 1394−1395.
(94) Verheijen, M.; et al. DMSO induces drastic changes in human cellular processes and epigenetic landscape in vitro. *Sci. Rep.* **2019**, *9*, 4641.
(95) Stolzing, A.; Naaldijk, Y.; Fedorova, V.; Sethe, S. Hydroxyethylstarch in cryopreservation - Mechanisms, benefits and problems. *Transfus. Apher. Sci.* **2012**, *46*, 137−147.
(96) Robles, V.; Valcarce, D. G.; Riesco, M. F. The use of antifreeze proteins in the cryopreservation of gametes and embryos. *Biomolecules* **2019**, *9*, 181.
(97) Ekpo, M. D.; et al. Antifreeze Proteins: Novel Applications and Navigation towards Their Clinical Application in Cryobanking. *Int. J. Mol. Sci.* **2022**, *23*, 2639.
(98) Knight, C. A.; Wen, D.; Laursen, R. A. Nonequilibrium antifreeze peptides and the recrystallization of ice. *Cryobiology* **1995**, *32*, 23−34.
(99) Biggs, C. I.; et al. Mimicking the Ice Recrystallization Activity of Biological Antifreezes. When is a New Polymer "Active"? *Macromol. Biosci.* **2019**, *19*, No. 1900082.

https://doi.org/10.1021/acs.chemmater.4c00266
Chem. Mater. 2024, 36, 3424−3434